Available online at www.sciencedirect.com
ScienceDirect
Journal of Solid State Chemistry 180 (2007) 2713–2722
JOURNAL OF SOLID STATE CHEMISTRY
www.elsevier.com/locate/jssc

New process of preparation, structure, and physicochemical investigations of the new titanyl phosphate $Ti_2O(H_2O)(PO_4)_2$

S. Benmokhtar[a,*], A. El jazouli[a], J.P. Chaminade[b], P. Gravereau[b], M. Ménétrier[b], F. Bourée[c]

[a]*LCMS, UFR Sciences des Matériaux Solides, Faculté des Sciences Ben M'Sik, Casablanca, Morocco*
[b]*Institut de chimie de la matière condensée de Bordeaux (ICMCB-CNRS UPR 9048), Université de Bordeaux 1, 87 Av. Dr. Schweitzer, 33608 Pessac, France*
[c]*Laboratoire Léon Brillouin, Saclay, France*

Received 22 February 2007; received in revised form 19 July 2007; accepted 25 July 2007
Available online 12 August 2007

Abstract

New titanyl phosphate $Ti_2O(H_2O)(PO_4)_2$ has been prepared and characterized by X-ray and neutron diffraction, nuclear magnetic resonance, infrared and Raman spectroscopies and thermogravimetric analysis. The crystal structure has been solved from neutron powder diffraction data at 300 K by Rietveld method in $P2_1$ space group. The refinement led to satisfactory profile factors ($R_p = 2.7\%$, $R_{wp} = 3.2\%$) and crystal structure model indicators ($R_B = 5.8\%$, $R_F = 3.2\%$). The cell is monoclinic with $a = 7.3735$ Å, $b = 7.0405$ Å, $c = 7.6609$ Å and $\beta = 121.48^\circ$, $Z = 4$. The structure can be described as a three-dimensional framework built up by chains of $[TiO_5(OH_2)]$ octahedra with alternative short bonds [$Ti_{(1)}$–$O_{(12)}$; $Ti_{(2)}$–$O_{(12)}$, 1.88–1.84 Å] and long ones [$Ti_{(1)}$–O_W; $Ti_{(2)}$–O_W, 2.25–2.23 Å] along *c*-axis and connected via $[PO_4]$ tetrahedra. Oxygen atom denoted $O_{(12)}$ is only linked to two titanium atoms and Oxygen atom denoted O_W is linked to two titanium atoms and two hydrogen atoms. $O_{(12)}$ and O_W are not linked to P atoms and justify the titanyl phosphate formulation $Ti_2O(H_2O)(PO_4)_2$. The infrared and Raman spectra presents peaks due to vibrations of Ti–O, P–O and O–H bonds. The ^{31}P MAS NMR spectrum reveals two ^{31}P resonance lines, in agreement with the structure which showed two crystallographic sites for phosphorus. The thermogravimetric analysis show that $Ti_2O(H_2O)(PO_4)_2$ is thermally stable until 400 °C. Above this temperature, it losses water and decomposes to $Ti_5O_4(PO_4)_4$ and TiP_2O_7.

Keywords: Synthesis; Titanyl phosphate; X-ray diffraction; Neutrons; Raman; Infrared; NMR

1. Introduction

Titanyl phosphates compounds of general stoichiometry $M(TiO)PO_4$ ($M = K$, Rb, Tl, Cs) have gained great importance in the last three decades in the field of communication and laser technology [1–5]. One of the most important titanyl phosphates is $K(TiO)PO_4$ (KTP). It is unique in its overall qualifications for second-order nonlinear and electrooptic processes [6], since then many researchers have focused their studies on KTP and its isostructural analogs. All members of this family are orthorhombic, biaxial crystals and belong to the noncentrosymmetric space group $Pna2_1$ (point group *mm*2). In general, the structure of the titanyl phosphates has the same type of framework and contains interoctahedral Ti–O–Ti bonds, resulting in infinite octahedral chains of corner-sharing $[TiO_6]$ octahedra and alkali metal atoms orderly situated between the chains. The Ti–O bonds inside the octahedra are not equal to each other: there are four close equatorial distances about 2 Å, one shortened due to a titanyl bond formation of an apical distance (about 1.7 Å) and one elongated (opposite to titanyl distance) with a bondlength greater than 2 Å.

Nowadays there are number of reports on synthesis and investigation of titanyl compounds. Among them, the most interesting works are on titanyl phosphates, titanyl arsenates of chemical formulas $M^{II}_{0.50}(TiO)XO_4$ and $Li_{1-2x}M_x^{II}(TiO)XO_4$ ($X = P$, As, $M^{II} = Mg$, Fe, Co, Ni, Cu, Zn) [7–12], titanyl silicates $Ca(TiO)SiO_4$ [13,14], $M_2(TiO)SiO_4$ ($M = Na$, Li) [15–17], titanyl germanate

*Corresponding author. Fax: +212 22704675.
E-mail addresses: s.benmokhtar@univh2m.ac.ma, sbenmokhtar@yahoo.com (S. Benmokhtar).

0022-4596/$ - see front matter © 2007 Elsevier Inc. All rights reserved.
doi:10.1016/j.jssc.2007.07.028

$Ca(TiO)GeO_4$ [18]. In addition, many compounds with open structures have been structurally determined up to now since the discovery of the layered titanium metal phosphates with the general formulas $\alpha Ti(HPO_4)_2 \cdot H_2O$ and $\gamma Ti(PO_4)(H_2PO_4) \cdot 2H_2O$ [19] for their interesting properties as catalysts and ionic conductors, selective ion exchangers, materials for nonlinear optics, intercalation, radioactive waste hosts and adsorbent of toxic heavy metal ions [20–24]. During our search for new compounds in the ternary system TiO_2–P_2O_5–H_2O resulted in the discovery of a new titanyl phosphate $Ti_2O(H_2O)(PO_4)_2$ (i.e., $P_2O_5 \cdot 2TiO_2 \cdot H_2O$). The aim of this work is to report on the synthesis, crystal structure, NMR, IR and Raman spectroscopies and TGA. The structural study of the compound was carried out using Rietveld profile method from the powder Neutron diffraction data.

2. Experimental

2.1. Synthesis

The $Ti_2O(H_2O)(PO_4)_2$ (denoted by TiHP) compound was synthesized using two procedures. In both methods we used $Cu_{0.50}(TiO)PO_4\alpha$ as starting material prepared according to the method given by Benmokhtar et al. [9].

2.1.1. Method I: exchange reaction Cu^{2+}/H^+ under mild hydrothermal conditions

$Ti_2O(H_2O)(PO_4)_2$ was obtained by ion-exchanging the $Cu_{0.50}(TiO)PO_4\alpha$ powder in a diluted aqueous solution of HNO_3 (2 N) at 230 °C, for at least 72 h, in a Teflon-lined steel autoclave under autogenous pressure. This ion-exchange procedure was performed three times (Fig. 1). The final product was filtered off, washed with distilled water and dried at 200 °C. The synthesis reaction is as follows:

$$2Cu_{0,5}(TiO)PO_4\alpha(s) + 2HNO_3(aq) \rightarrow Ti_2O(H_2O)(PO_4)_2(s) + Cu^{2+}(aq) + 2NO_3^-\ (aq).$$

The material prepared by this method contained very small amounts of some unidentified impurity. These few extra peaks have relatively low intensity (<1%); therefore we have thought about a new method.

2.1.2. Method II: thermal treatment of $Cu_{0.50}(TiO)PO_4\alpha$ in reducing atmosphere

$Ti_2O(H_2O)(PO_4)_2$ was prepared by reduction of $Cu_{0.5}TiO(PO_4)\alpha$ at 400 °C for 24 h in reducing atmosphere (5% H_2 + 95% Ar) then cooled in the same atmosphere at ambient temperature according to the reaction:

$$2Cu_{0,5}(TiO)PO_4\alpha(s) + H_2(g) \rightarrow Ti_2O(H_2O)(PO_4)_2(s) + Cu(s).$$

The X-ray powder diffraction (XRPD) data of the resulting product (red colour) shows the presence of TiHP and Cu (Fig. 2). Cu was eliminated by leaching with dilute solution of HNO_3. After filtrating, the sample was washed with distilled water and dried at room temperature. In these conditions a pure phase TiHP (white colour) is obtained. All the characterizations have been done on the sample obtained by second method.

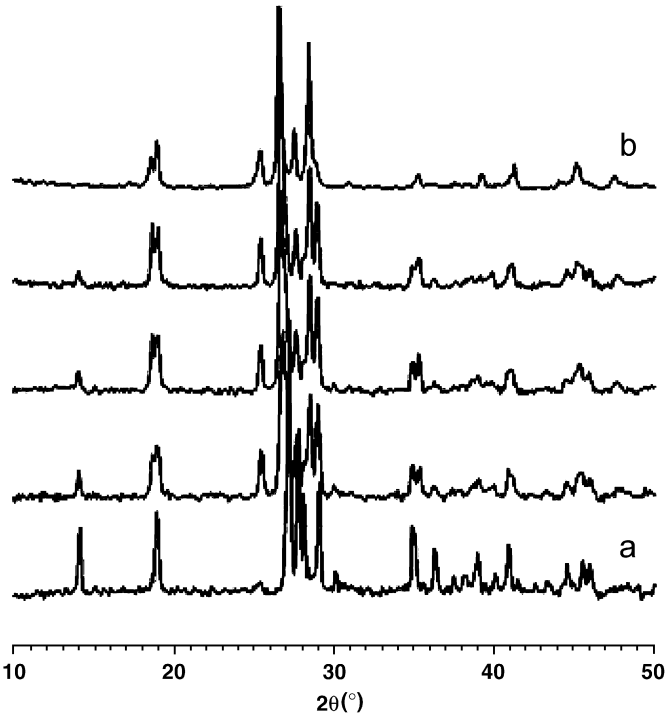

Fig. 1. X-ray powder patterns at room temperature of $Ti_2O(H_2O)(PO_4)_2$ (b) prepared by ion-exchanging the $Cu_{0.50}(TiO)PO_4\alpha$ (a) powder in a diluted aqueous solution of HNO_3 (2 N) at 230 °C.

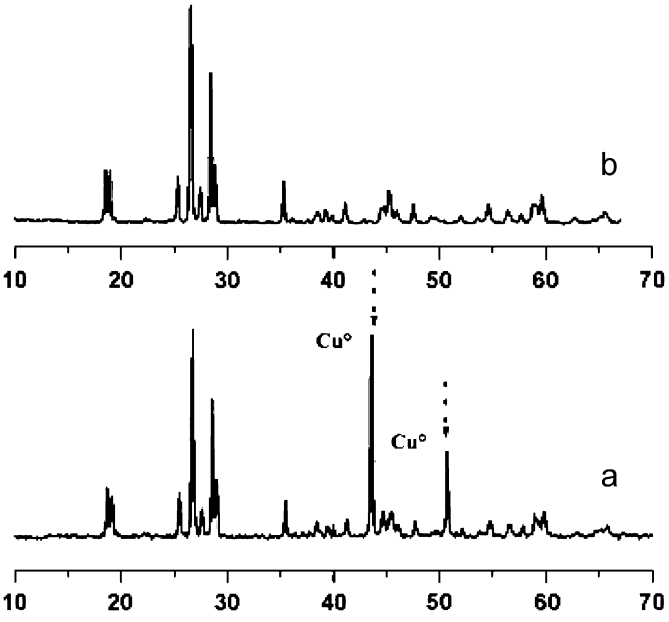

Fig. 2. X-ray powder patterns at room temperature of $Ti_2O(H_2O)(PO_4)_2$ prepared by thermal treatment in reducing atmosphere , before (a) and after (b) leaching.

Efforts to grow single crystals have been performed by hydrothermal method in the system TiO_2–P_2O_5–H_2O starting from TiO_2 and H_3PO_4. Single crystals have been obtained but the composition do not match $Ti_2O(H_2O)(PO_4)_2$ formula, characterization of these crystals is in progress.

2.2. Instrumental analysis

The XRPD data were collected at room temperature with a Philips PW 3040 ($\theta-\theta$) diffractometer using a graphite monochromator.

Neutron diffraction data have been collected at room temperature on the high resolution powder diffractometer 3T2 in Saclay (LLB, Orphée Reactor), with: $\alpha_1 = 10'$; vertically focusing Ge (335) monochromator; $\lambda = 1.2251$ Å; 6–125.70° angular range of measurement (2θ), 0.05° step; $20He^3$ detectors, $\alpha_3 = 10'$.

^{31}P and ^{1}H NMR spectra were obtained at room temperature on a Bruker AVANCE 300 spectrometer. The ^{31}P spectrum was taken at a spinning rate of 10 kHz (4 mm rotor) using a single pulse sequence. Chemical shifts were determined using 85% H_3PO_4 as a reference (0 ppm).

The Raman spectrum was recorded under the microscope of a Dilor XY Multichannel spectrometer. Excitation was accomplished with the 514.5 nm line of an argon-ion laser. Incident power was approximately 100 mW at the source of which only 10% hit to the sample.

The infrared spectra were recorded using a Bruker IFS 113 v FT-IR spectrometer. Samples were in the form of KBr (mid-IR) and polyethylene (far-IR) pellets.

TGA were performed with a Setaram TGDTA92 thermogravimetric analyzer at a rate of 2 °C min^{-1} in air from room temperature to 650 °C with a final thermal plateau at this temperature for 1 h.

3. Structure determination

A structure determination using the Rietveld method from powder data was performed in two principle models. In the first model the refinement was made in $P2_1/c$ space group (No. 14) whereas in the second the hypothesis of $P2_1$ (No. 4) was verified.

First searches were done for a structural model of monoclinic symmetry derived from $Mg_{0.50}(TiO)PO_4$ [10]. H atoms were excluded. Carefully analysis of the results showed that few weak calculated reflections did not fit well with the observed ones. These weak peaks were not due to supercell reflections. As can easily be seen, the space group $P2_1/c$ is not compatible with the observed diffraction pattern. As will be discussed in the following the ^{31}P MAS NMR study was carried out to give local information. The study of ^{31}P MAS NMR of $Mg^{II}_{0.50}(TiO)PO_4$ [10] has shown only a single ^{31}P resonance line. But the study of ^{31}P MAS NMR of TiHP has shown two ^{31}P resonance lines. This suggests the existence of two crystallographic sites for phosphorus in the structure. These problems led us to reconsider the starting hypothesis for this compound.

In the second model, an ab initio structure determination from X-ray powder data was performed. The powder diffraction pattern was indexed with Dicvol 91 program [25]. A monoclinic solution was found with satisfactory figures of merit ($M(20)/F(20) = 23$ and 37 (0.0108, 50)) and systematic absences ($0\,k\,0$ ($k = 2n+1$) were consistent with the space group $P2_1$ (No. 4) and the indexed powder pattern is reported in Table 1. The symmetry information and the unit cell parameters were then input to Fullprof program [26] to decompose the pattern. Total 931 values of $|F_{obs}|$ were extracted. The profile matching factors corresponding to $P2_1$ converged to the values $R_{wp} = 12.7\%$, $R_{exp} = 5.39\%$. The density of the TiHP was measured to be 3.10 g/cm^3. According to this result and the symmetry information, it is determined that there are four $Ti_2O(H_2O)(PO_4)_2$ molecules per unit cell.

Direct methods were applied with Shelxs-86 program [27] to $|F_{obs}|$ obtained using Fullprof program [26]. The list of interatomic distances showed that 5 of the 12 peaks

Table 1
X-ray powder diffraction data of monoclinic $Ti_2O(H_2O)(PO_4)_2$

$h\,k\,l$	d_{obs} (Å)	d_{calc}(Å)	$100I/I_0$
−1 1 1	4.795	4.796	64
1 1 0	4.688	4.689	37
−1 1 2	3.364	3.365	33
−2 0 2	3.226	3.227	21
0 0 −2	3.264	3.266	23
1 1 1	3.255	3.256	23
2 0 0	3.143	3.144	17
0 2 1	3.097	3.099	25
−2 2 −1	2.543	2.544	28
2 0 3	2.503	2.504	4
−2 2 2	2.396	2.398	56
0 2 2	2.392	2.394	56
−1 1 3	2.355	2.356	18
2 2 0	2.344	2.345	100
−3 1 2	2.300	2.300	39
1 1 2	2.293	2.294	38
−3 1 1	2.265	2.265	6
−1 3 1	2.210	2.209	22
1 3 0	2.197	2.198	6
−3 1 3	2.084	2.085	19
−2 2 3	2.040	2.040	14
3 1 0	2.018	2.018	10
−1 3 2	2.00	2.000	6
1 3 1	1.976	1.977	10
2 2 1	1.975	1.975	23
−2 0 4	1.915	1.915	8
0 2 −3	1.852	1.852	14
1 1 3	1.734	1.734	16
−3 3 2	1.689	1.689	16
1 3 2	1.687	1.687	16
−2 2 4	1.682	1.682	37
−4 2 3	1.598	1.598	14
4 0 0	1.572	1.572	26
−4 2 1	1.567	1.567	13
2 4 0	1.535	1.535	11
−5 1 3	1.440	1.440	12
4 2 0	1.435	1.435	11
1 3 3	1.423	1.423	9

listed in the E-map were likely to correspond to the correct positions of atoms. The strongest one of the five peaks was assigned to Ti, the weakest $P_{(1)}$ and the remaining $O_{(22)}$–$O_{(31)}$ according to the interatomic distances. The other atoms were located by using difference Fourier synthesis with Shelxl-93 [28] and approximate $|F_{obs}|$ values derived by the pattern decomposition method. In this course, once an atom was located, it would be used for the next run of difference-Fourier synthesis. Considering that the neutron diffraction is more sensitive to the hydrogen, Rough structure obtained by using direct methods and difference-Fourier synthesis was refined from the neutron powder diffraction data with the Rietveld method [29]. Refinement involved the following parameters: one scale factor, 48 atomic coordinates, four isotropic temperature factor, one zero point and four cell parameters, three half-width parameters, one asymmetry factors, one parameter to define the θ-dependent pseudo-Voigt profile shape function, five coefficients to describe the functional dependence of the background and one preferred orientation factor. Details of the structure determination are summarized in Table 2. The final agreement factors are satisfactory: $R_p = 2.7\%$, $R_{wp} = 3.2\%$ and $R_B = 5.8\%$, $R_F = 3.2\%$. The final Rietveld plot of the refined structure is shown in Fig. 3. Atomic coordinates are reported in Table 3 while bond distances and angles are given in Table 4.

Table 2
Crystal data and refinement parameters for $Ti_2O(H_2O(PO_4)$

Crystal data	
Cell setting	Monoclinic
Space group	$P2_1$
a (Å)	7.3735(12)
b (Å)	7.0405(10)
c (Å)	7.6609(10)
β (°)	121.48(2)
Volume (Å^3)	339.2(1)
Z	4
d_{calc} (g/cm^3)	3.13
$d_{meas.}$ (g/cm^3)	3.10
Refinement	
Diffractometer	3T2 (réacteur Orphée, LLB)
Wavelength (Å)	1.2251
Profile range (°2θ)	6.0–125.7
Step size (°2θ)	0.05
Number of reflections	1271
Number of refined parameters	67
Pseudo-Voigt function	
PV = $\eta L + (1-\eta)G$	$\eta = 0.29(14)$
Half-width parameters	$U = 0.56(7)$; $V = -0.58(7)$; $W = 0.26(2)$
R_F (%)	3.2
R_B (%)	5.8
Rp (%)	2.7
Rwp (%)	3.2
cRp[a] (%)	13.9
cRwp[a] (%)	12.7
χ^2	3.69

[a]Conventional factors without background.

4. Results and discussion

4.1. Description of the structure

The architecture of a three-dimensional (3D) framework of $Ti_2O(H_2O)(PO_4)_2$ titanyl phosphate is very close to those for titanyl phosphates: $Na(TiO)PO_4$ [30] and especially $Li(TiO)PO_4$ (*Pnma* (No. 62)) [31] which shows a similar framework-building $TiPO_5$ based on $[TiO_6]$ octahedra and $[PO_4]$ tetrahedra. The dominant structural units are chains of tilted corner-sharing $[TiO_6]$ octahedra which run parallel to c in $Ti_2O(H_2O)(PO_4)_2$ and a-axis in $Li(TiO)PO_4$. Chains are linked by phosphate tetrahedra to constitute sheets.

The framework of $Ti_2O(H_2O)(PO_4)_2$ is made of corner-sharing titanium octahedra and isolated tetrahedral phosphate groups. The $[TiO_5(OH_2)]$ octahedra are linked by $[PO_4]$ tetrahedra and the large cavities formed by this framework are unoccupied (Fig. 5). $Ti_{(1)}$ and $Ti_{(2)}$ octahedra alternate along the [001] direction to form infinite chains –Ti–O(H_2)–Ti–O–Ti–O(H_2)–Ti– of linked $[TiO_5(OH_2)]$ octahedra (Fig. 4). The $[TiO_5(OH_2)]$ octahedra show their typical KTP-type distortion mode, in which the titanium atom makes a nominal displacement from the center of its octahedron along a Ti–O bond axis, which results in long bonds formed between Ti(1) and O_W and Ti(2) and O_w [$Ti_{(1)}$–O_W; $Ti_{(2)}$–O_W, 2.25–2.23 Å]. Each Ti center makes two Ti–O–Ti′ bonds via O_w and $O_{(12)}$ and four Ti–O–P bonds. The $O_{(12)}$ is only linked to two titanium atoms and O_W (O water) is linked to two titanium atoms and two hydrogen atoms, they are independent because they do not belong to the $[PO_4]$ groups and justify the titanyl phosphate of formulation $Ti_2O(H_2O)(PO_4)_2$. A simple measure of the degree of distortion, Δ(Ti) of the two distinct $[TiO_5(OH_2)]$ entities in $Ti_2O(H_2O)(PO_4)_2$ using the equation $\Delta = 1/6\sum_1^6\{(r_n - \langle r\rangle)/\langle r\rangle\}^2$ where r_n and $\langle r\rangle$ are the individual and average bond lengths, respectively [32] gives $\Delta_{Ti} \times 10^4 = 50$ for Ti(1) and Δ_{Ti}. $10^4 = 58$ for Ti(2) which is nearly the same as the one determined for $LiTiO(PO_4)$ ($\Delta_{Ti} \times 10^4 = 69$) [31] but higher than the value found for TiO_2 (rutile) ($\Delta_{Ti} \times 10^4 = 6$) or $M_{0.50}Ti_2(PO_4)_3$ Nasicon type ($M = Mg$, $\Delta_{Ti} \times 10^4 = 36$ [33]; $M = Co$, $\Delta_{Ti} \times 10^4 = 37$) [34], reflecting the higher instability of Ti^{4+} cations in $Ti_2O(H_2O)(PO_4)_2$ titanyl phosphate.

There are two crystallographic phosphorus sites. Both are tetrahedrally bonded to four O atoms and share its oxygen atoms with four $[TiO_5(OH_2)]$ groups in three separate chains. As usually observed for orthophosphate groups, there is one type of P–O distances inside the $[PO_4]$ tetrahedron. The average values for the P–O distances and P–O–P angles are (1.537(5) Å, 109.36 (26)°) and (1.532(5) Å, 109.45(29)°), respectively for $[P_{(1)}O_4]$ and $[P_{(2)}O_4]$ tetrahedra. The average values for the corresponding O–O distances inside the $[PO_4]$ tetrahedral are of the same order 2.51(3) Å. All these distances and angles are in accordance with previous observations of $[PO_4]$ tetrahedra involved in other orthophosphate anions [7–10,34–36].

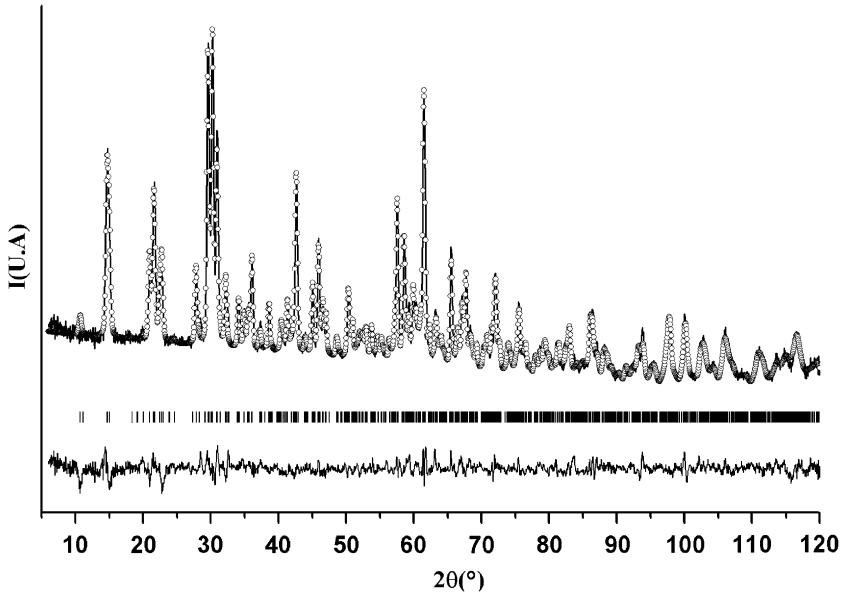

Fig. 3. Experimental (◦◦◦◦◦), calculated (—), and difference profile of the neutrons diffraction pattern of $Ti_2O(H_2O)(PO_4)_2$.

Table 3
Atomic coordinates and isotropic temperature factors in $Ti_2O(H_2O)(PO_4)_2$

Atom	Site	x	y	z	B_{iso} (Å^2)
Ti(1)	2*a*	0.7436(51)	0.2678	0.7210(39)	0.1
Ti(2)	2*a*	−0.7495(40)	−0.2126(50)	−0.2710(40)	0.1
P(1)	2*a*	0.2465(31)	0.1333(37)	0.9839(27)	0.21(11)
P(2)	2*a*	−0.2450(38)	−0.1240(39)	−0.4955(40)	0.21(11)
O_W	2*a*	0.7585(37)	0.1636(37)	0.0069(33)	0.38(4)
O(12)	2*a*	−0.7416(32)	−0.1251(38)	−0.4943(37)	0.38(4)
O(21)	2*a*	0.7652(31)	0.0049(39)	0.3395(27)	0.38(4)
O(22)	2*a*	−0.7419(34)	0.0164(44)	0.1655(27)	0.38(4)
O(31)	2*a*	0.4502(31)	0.2565(40)	0.0887(26)	0.38(4)
O(32)	2*a*	−0.4474(33)	−0.2418(38)	−0.5963(28)	0.38(4)
O(41)	2*a*	0.2546(33)	0.0141(41)	0.8335(25)	0.38(4)
O(42)	2*a*	−0.2417(35)	0.0176(40)	−0.3399(25)	0.38(4)
O(51)	2*a*	0.0560(35)	0.2438(44)	0.4028(30)	0.38(4)
O(52)	2*a*	−0.0484(35)	−0.2280(37)	0.1089(26)	0.38(4)
H(1)	2*a*	0.6475(32)	0.0161(48)	0.9472(43)	2.76(33)
H(2)	2*a*	0.9062(37)	0.0797(44)	0.0787(48)	2.76(33)

In the HTiP compound, the water molecules are coordinated to the titanium, a strong hydrogen bonds exist between hydrogen atoms of the water groups (O_W) and oxygen atoms of the inorganic framework but only two H-bonds between different chains could be considered according to the values of distances and angles: O_w–H(2)···O(52) (O_w–H(2): 1.10 Å; H(2)···O(52): 2.19 Å; angle O_w–H(2)···O(52): 130°), O_w–H(1)···O(31) (O_w–H(1): 1.25 Å; H(1)···O(31): 1.93 Å; angle O_w–H(1)···O(31): 164°). In case of the long distance H···O, the strength of the H-bond will be too weak for being considered. Most of these bonds are illustrated in Fig. 5. These hydrogen bonds ensure the stability of the structure.

Note that this new structure do not belong to the layered structures found in the system TiO_2–P_2O_5–H_2O.

4.2. NMR study

4.2.1. ^{31}P NMR

Several reports in the literature suggest that ^{31}P MAS NMR spectra exhibit separate signals for crystallographically different phosphorus atoms in titanium phosphates structures. For example in the Nasicon type, Young and Wenqin [35] report that for $NaTi_2(PO_4)_3$, the ^{31}P MAS NMR spectrum show only one peak at ∼−27 ppm, which is consistent with the occupation by the phosphorus atoms of the 18*e* position of the rhombohedral $R\bar{3}c$ SG. Also Sobha and Rao [37] report that the spectrum of $Na_5Ti(PO_4)_3$ presents two peaks ∼0 and ∼−5 ppm corresponding to two crystallographically distinct positions (9*d* and 9*c*) for the phosphorus atoms in the rhombohedral *R*32 SG. On the other hand, in the titanyl phosphates type, we have recently reported [10] that for the $Mg_{0.50}(TiO)PO_4$ and $Li(TiO)PO_4$, the ^{31}P MAS NMR spectra for both compound show only one peak, which is consistent with the occupation by the phosphorus atoms of the 4*e* position of monoclinic $P2_1/c$ SG for $Mg_{0.50}(TiO)PO_4$ (∼−20 ppm), and 4*c* position of orthorhombic *Pnma* SG for $Li(TiO)PO_4$ (∼−11 ppm).

In the present study, ^{31}P MAS NMR was used for $Ti_2O(H_2O)(PO_4)_2$ and $K(TiO)PO_4$, the spectra (Fig. 6) display two resonance lines at ∼−9 and ∼−31 ppm for $Ti_2O(H_2O)(PO_4)_2$ and at ∼0 and ∼−1 ppm for $K(TiO)PO_4$. This suggests the existence of two crystallographically inequivalent or differently coordinated phosphorus atoms in the materials, which is in agreement with the crystallographic data in space group $P2_1$ and $Pna2_1$ [2]. Note that

Table 4
Interatomic distances (Å) and angles (°) in $Ti_2O(H_2O)(PO_4)_2$

$Ti(1)O_6$	O_W	O(12)	O(22)	O(32)	O(42)	O(52)
O_W	**2.25(3)**	175.01(24)	82.44(19)	86.33(20)	87.45(18)	84.25(22)
O(12)	4.13(3)	**1.88(3)**	93.01(20)	95.68(25)	97.00(22)	93.55(22)
O(22)	2.78(3)	2.78(3)	**1.95(3)**	89.03(22)	169.69(27)	87.81(23)
O(32)	2.83(3)	2.78(3)	2.68(3)	**1.87(4)**	92.46(24)	170.39(29)
O(42)	2.84(3)	2.79(3)	3.70(4)	2.68(3)	**1.84(2)**	89.05(22)
O(52)	3.01(3)	2.77(3)	2.68(3)	3.78(3)	2.63(3)	**1.92(4)**

$Ti(2)O_6$	O_W	O(12)	O(21)	O(31)	O(41)	O(51)
O_W	**2.23(2)**	176.55(21)	80.16(19)	82.13(21)	86.78(23)	80.44 (19)
O(12)	4.08(4)	**1.84(3)**	96.49(24)	97.58(22)	96.65(24)	99.23(25)
O(21)	2.75(3)	2.90(3)	**2.04(4)**	88.06 (22)	166.85(30)	79.65(22)
O(31)	2.73(3)	2.82(3)	2.74(3)	**1.90(3)**	91.76(25)	160.14(26)
O(41)	2.77(3)	2.70(3)	3.79(4)	2.65(3)	**1.77(4)**	96.68(25)
O(51)	2.71(3)	2.89(4)	2.56(3)	3.81(4)	2.79(3)	**1.95(4)**

$P(1)O_4$	O(22)	O(31)	O(41)	O(52)
O(22)	**1.58(3)**	104.14(28)	113.11(21)	109.21(26)
O(31)	2.46(3)	**1.54(3)**	107.73(27)	107.77(27)
O(41)	2.53(2)	2.42(3)	**1.45(3)**	114.21(30)
O(52)	2.57(3)	2.52(3)	2.54(3)	**1.58(3)**

$P(2)O_4$	O(21)	O(32)	O(42)	O(51)
O(21)	**1.58(3)**	110.46(30)	104.86(25)	108.10(29)
O(32)	2.55(3)	**1.51(3)**	111.10(29)	108.84(31)
O(42)	2.48(2)	2.52(3)	**1.54(3)**	113.35(33)
O(51)	2.50(3)	2.46(3)	2.55(4)	**1.50(4)**

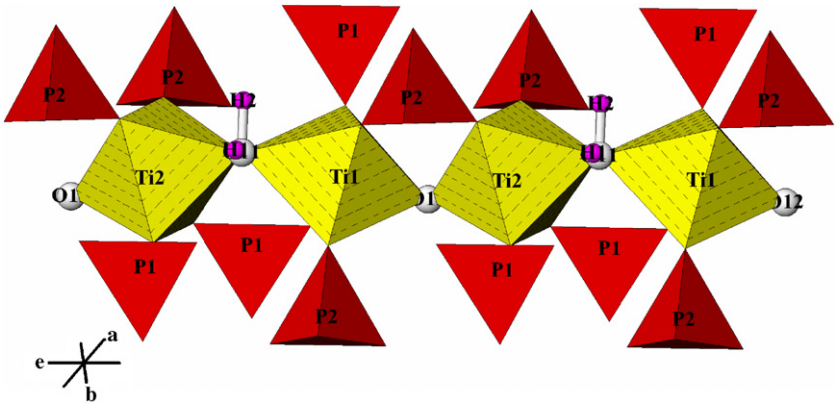

Fig. 4. –Ti–O(H_2)–Ti–O–Ti–O(H_2)–Ti– chains in $Ti_2O(H_2O)(PO_4)_2$.

the NMR results of KTP are similar to those reported previously [38].

4.2.2. ^1H NMR

The NMR ^1H spectrum of the $Ti_2O(H_2O)(PO_4)_2$ was obtained after heating the sample in a vacuum oven at 120 °C overnight to remove as much of the absorbed water as possible. The spectrum (Fig. 7) show a central line at ~0 ppm and clearly demonstrate Pake's doublet that results from the mutual dipolar interaction of closely spaced, isolated proton pairs, indicating the existence of water molecules in the compound.

4.3. Infrared and Raman spectroscopy

The infrared and Raman spectra of the $Ti_2O(H_2O)(PO_4)_2$ are shown in Fig. 8. The frequencies of the observed bands along with the assignments are given in Table 5.

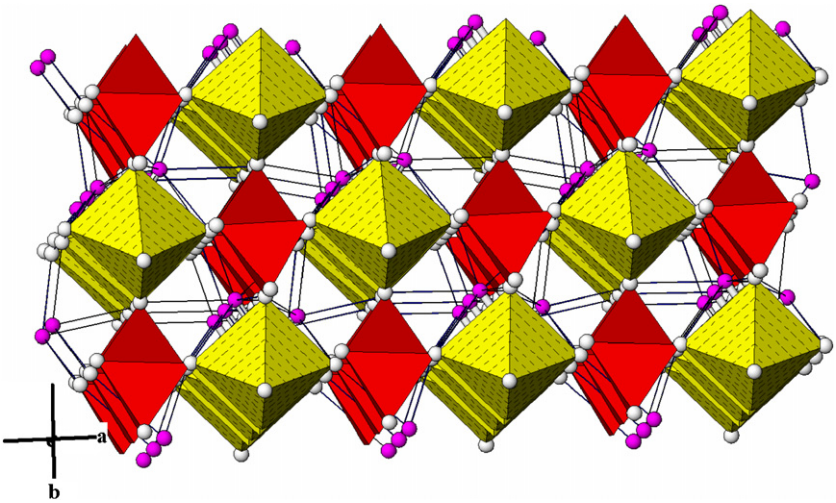

Fig. 5. Projection of the structure of $Ti_2O(H_2O)(PO_4)_2$ along the c axis. The [TiO_6] and [PO_4] groups are represented by polyhedra (H-bonds are represented by dotted lines).

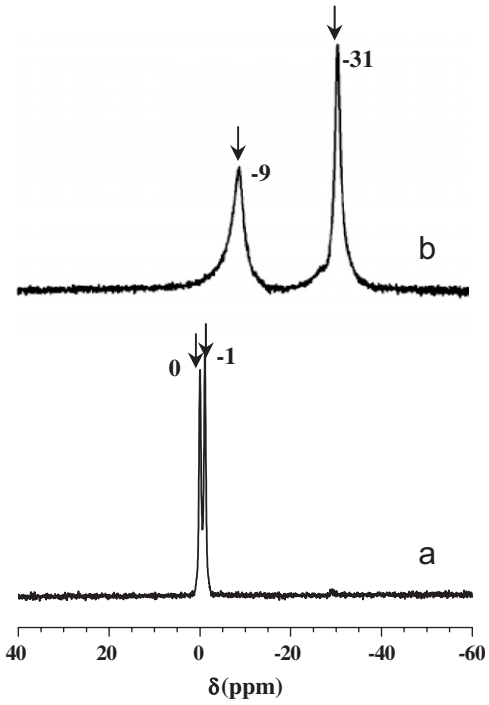

Fig. 6. Comparison of ^{31}P MAS NMR spectra in titanyl phosphate $K(TiO)PO_4$ (a) and $Ti_2O(H_2O)(PO_4)_2$ (b).

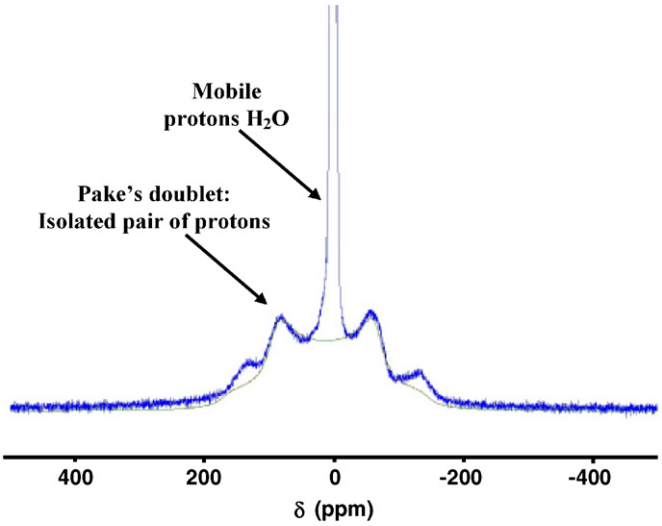

Fig. 7. ^1H static NMR spectrum for $Ti_2O(H_2O)(PO_4)_2$.

4.3.1. *Infrared*

The phosphate units are characterized by four main domains in the IR spectrum. They correspond to the antisymmetric stretching mode (νas) between 1000 and 1250 cm^{-1}, the symmetric stretching mode (νs) from 900 to 1000 cm^{-1}, the antisymmetric bending mode (δas) from 500 to 700 cm^{-1} and the symmetric bending mode (δs) between 300 and 500 cm^{-1}. Consequently, for the compound, the bands located between 1010 and 1185 cm^{-1} were assigned to the triply degenerate νas(PO_4) while that observed near 962 cm^{-1} was attributed to νs(PO_4) in the domain of stretching vibration modes (Table 5). In the domain of the bending modes, the bands were attributed to the doubly degenerate δs(PO_4) (between 383 and 461 cm^{-1}) and to the triply degenerate δas(PO_4) (between 492 and 628 cm^{-1}) modes.

The presence of the bands at around 1651, 1514 cm^{-1} (narrow) and 3256 cm^{-1} (broad) associated to the bending and stretching modes of water molecule, respectively, confirmed the presence of molecule water in titanyl phosphate, as expected from the ATG results.

4.3.2. *Raman*

The Raman spectrum of $Ti_2O(H_2O)(PO_4)$ is reported in Fig. 8. The high frequency part (900–1100 cm^{-1}) exhibits six bands (1087, 1050, 1015, 1006, 972 and 904 cm^{-1}) (Table 5). These bands correspond to the stretching

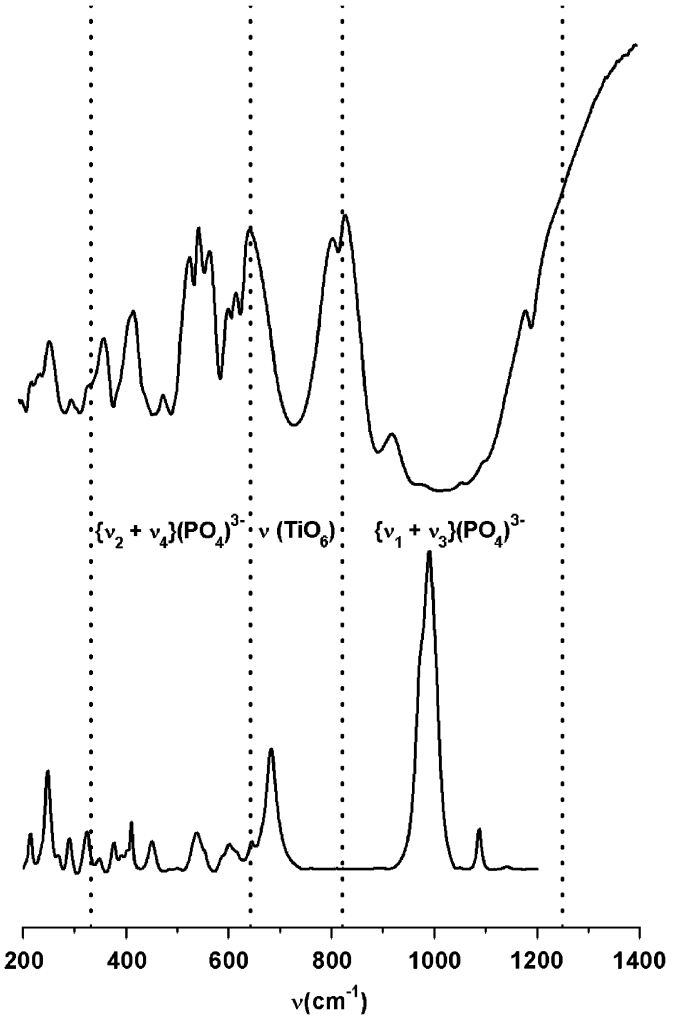

Fig. 8. Raman and Infrared spectra of $Ti_2O(H_2O)(PO_4)_2$.

Table 6
Description of the chemical bonds in the titanyl compounds

Compounds	Short length (Å)	ν_{TiO6}(cm^{-1})	Ref
$Ti_2O(H_2O)(PO_4)_2$	1.84	681	This work
$Fe_{0.50}(TiO)PO_4$	1.73	744	[8]
$Ni_{0.5}(TiO)PO_4$	1.70	750	[39]
$Li(TiO)PO_4$	1.70	783	[31]
$Na(TiO)PO_4$	1.70	745	[30]
$K(TiO)PO_4$	1.72	698	[40]
$Na_4(TiO)(PO_4)_2$	1.93	687	[30]
$(TiO)_2P_2O_7$	1.76	719	[41]
$Li(TiO)AsO_4$	1.70	769	[42]

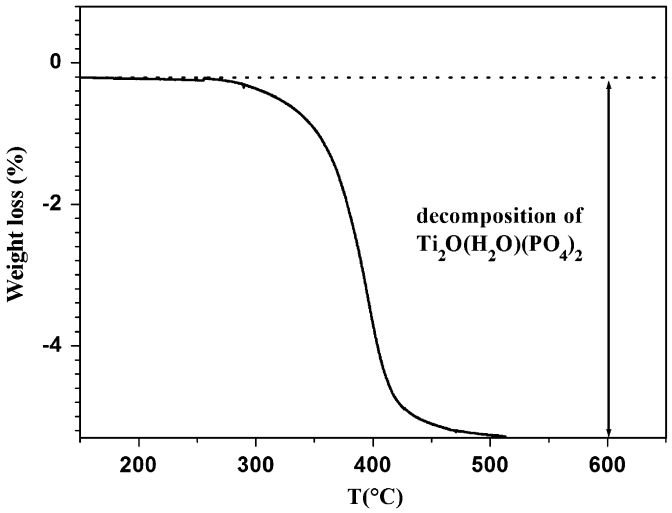

Fig. 9. TGA curve of the $Ti_2O(H_2O)(PO_4)_2$ (heating rate: 2 °C min^{-1} in air).

Table 5
Raman and infrared bands and assignments for the titanyl phosphate $Ti_2O(H_2O)(PO_4)_2$

Assignments	Bands (cm^{-1})	
	IR	Raman
Stretching modes of H_2O $\nu_{(O-H)}$	3256	
Deformation modes of H_2O $\delta_{(H-O-H)}$	1651, 1514	
Stretching modes $\nu_{(P-O)}$	1110, 1064, 1028, 1010, 962, 896	1087, 1050, 1015, 1006, 972, 904
Stretching mode $\nu_{(Ti-O)}$	727	681
Deformation modes $\delta_{(O-P-O)}$	628, 608, 594, 559, 536, 492, 461, 442, 383	642, 614, 601, 585, 536, 498, 451, 410, 376
Translational vibrations of the Ti^{4+}, and PO_4^{3-} ions and PO_4^{3-} librations	338, 323, 287, 242, 228, 196, 130	348, 323, 287, 268, 245, 213

vibrations of the PO_4 tetrahedra. The band observed at 681 cm^{-1} can be reasonably assigned to Ti–O single-bond vibration and this group is likely to be present in titanyl phases. In previous Raman studies many authors reported that titanyl phosphates, titanyl arsenates and titanyl pyrophosphates show the presence of a strong band in 700–800 cm^{-1} region that confirmed the existence of the infinite chains –Ti–O–Ti–O–Ti– in the structure (Table 6). For the P–O bending vibrations, nine Raman peaks (642, 614, 601, 585, 536, 498, 451, 410 and 376 cm^{-1}) are observed (Table 5). The peaks situated below 300 cm^{-1} are attributed to the external modes.

4.4. Thermal stability

To study the thermal stability, we heated $Ti_2O(H_2O)(PO_4)_2$ up to 650 °C and then analyzed the product by XRPD. The thermal gravimetric analysis (TGA) curve (Fig. 9) shows that a single state decomposition started at a temperature higher than 280 °C and ended at 600 °C, the total weight loss is equal to 5.2% which is comparable to the theoretical percentage calculated for the removal of water moles from the $Ti_2O(H_2O)(PO_4)$ (5.6%). This result is in good agreement with the water molecule determined by the structural study. Note that no weight loss

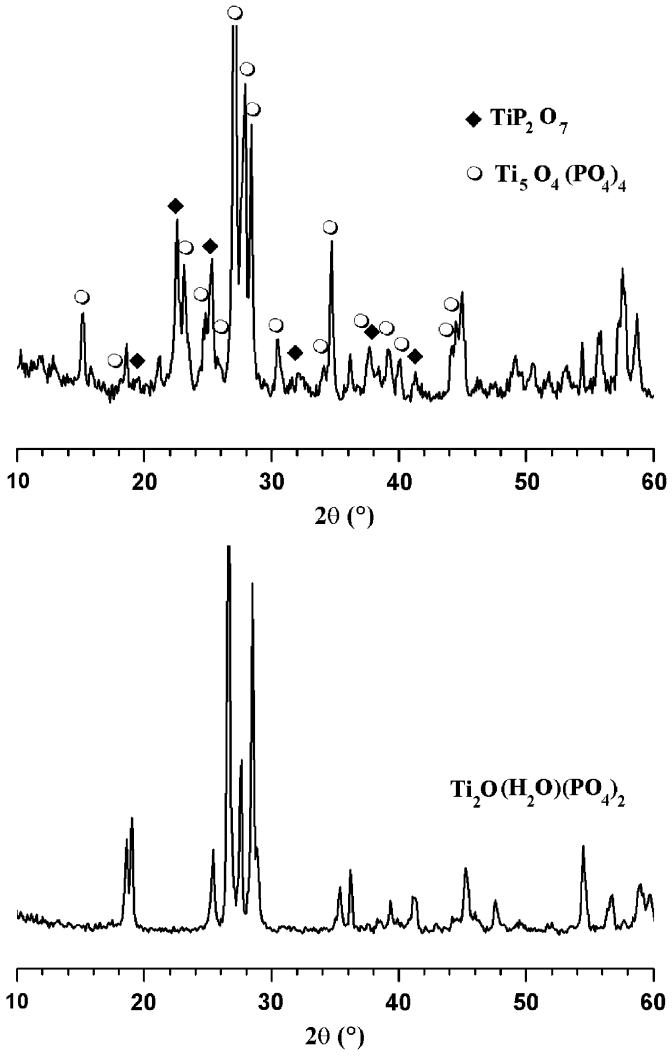

Fig. 10. Comparison of the XRPD patterns of the $Ti_2O(H_2O)(PO_4)_2$ at room temperature and after heating at 650 °C.

was observed below 400 °C, which indicates that no physiosorbed water is present in the compound. The analysis of XRPD (Fig. 10) showed a mixture of $Ti_5O_4(PO_4)_4$ and TiP_2O_7 *(PDF # 82-1340, 38-1468)* and the corresponding thermal transformation is as follows:

$$3Ti_2O(H_2O)(PO_4)_2 \rightarrow Ti_5O_4(PO_4)_4 + TiP_2O_7 + 3H_2O.$$

5. Conclusions

Powder of titanyl phosphate $Ti_2O(H_2O)(PO_4)$ has been prepared by thermal treatment of $Cu^{II}_{0,50}(TiO)PO_4\alpha$ under hydrogen-argon and by exchange reaction Cu^{2+}/H^+ under mild hydrothermal conditions. Its crystal structure has been resolved from powder neutrons diffraction data in $P2_1$ space group. It is constituted by chains of tilted corner-sharing $[TiO_5(OH_2)]$ octahedra running parallel to the *c*-axis and cross linked by $[PO_4]$ tetrahedra. Raman and IR spectra are consistent with the crystal structure for example, they show that stretching modes of $[PO_4]$ tetrahedra are observed at significantly higher frequency (900–1000 cm^{-1}) than stretching modes of $[TiO_6]$ groups (600–850 cm^{-1}). They also confirm the existence of infinite chains –Ti–O(H_2)–Ti–O–Ti–, like in the titanyl phosphate analog. Powder of $Ti_2O(H_2O)(PO_4)$ was also characterized by NMR spectroscopy and by thermogravimetric analysis. Results are in good agreement with structural data.

Acknowledgments

We wish to thank D. Denux for his contribution to the TGA measurements and subsequent interpretation, as well as E. Lebraud, S. Péchev and O. Viraphong for their technical support. We gratefully acknowledge Danita de Waal from the University of Pretoria South Africa, and more especially Bouchaib Manoun (Department of Chemistry, University of Pretoria South Africa) for assistance in obtaining the Raman and IR spectra. We are also grateful to ICMCB-CNRS France for support.

References

[1] J.D. Bierlein, H. Vanherzeele, J. Opt. Soc. Am. B 6 (4) (1989) 622.
[2] I. Tordjman, R. Masse, J.C. Guitel, Z. Kristallogr. 139 (1974) 103.
[3] G.D. Stucky, M.L.F. Phillips, T.E. Gier, Chem. Mater. 1 (5) (1989) 493.
[4] F.C. Zumsteg, J.D. Bierlein, T.E. Gier, J. Appl. Phys. 47 (1976) 4980.
[5] G.D. Stucky, M.L.F. Phillips, T.E. Gier, Chem. Mater. 1 (1989) 492.
[6] M.E. Hagerman, K.R. Poeppelmeier, Chem. Mater. 7 (1995) 602.
[7] P. Gravereau, J.P. Chaminade, B. Manoun, S. Krimi, A. El Jazouli, Powder Diffr. 14 (1999) 10.
[8] S. Benmokhtar, A. El Jazouli, J.P. Chaminade, P. Gravereau, A. Wattiaux, L. Fournès, J.C. Grenier, D. de Waal, J. Solid State Chem. 179 (2006) 3709.
[9] S. Benmokhtar, H. Belmal, A. El Jazouli, J.P. Chaminade, P. Gravereau, S. Péchev, J.C. Grenier, G. Villeneuve, D. deWaal, J. Solid State Chem. 180 (2007) 772.
[10] S. Benmokhtar, A. El Jazouli, S. Krimi, J.P. Chaminade, P. Gravereau, M. Ménétrier, D. deWaal, Mater. Res. Bull. 42 (2007) 892.
[11] B. Manoun, A. El Jazouli, P. Gravereau, J.P. Chaminade, F. Bouree, Powder Diffr. 17 (4) (2002) 290.
[12] B. Manoun, A. El Jazouli, P. Gravereau, J.P. Chaminade, Mater. Res. Bull. 40 (2005) 229.
[13] J.A. Speer, G.V. Gibbs, Am. Mineral. 61 (1976) 238.
[14] T. Malcherek, C. Paulmann, M.C. Domeneghetti, U. Bismayer, J. Appl. Crystallogr. 34 (2001) 108.
[15] A. Ziadi, G. Thiele, B. Elouadi, J. Solid State Chem. 109 (1994) 112.
[16] A. Ziadi, H. Hillebrecht, G. Thiele, B. Elouadi, J. Solid State Chem. 123 (1996) 324.
[17] H. Nyman, M. O'Keeffe, Crystallography B 34 (1978) 905.
[18] R. Ellemann-olesen, T. Malcherek, Am. Mineral. 90 (2005) 1325.
[19] A. Clearfield, J.A. Stynes, J. Inorg. Nucl. Chem. 26 (1964) 117.
[20] G. Alberti, M. Casciola, U. Costantino, D. Fabarani, in: E. Drioli, M. Nakagaki (Eds.), Membranes and Membrane Processes, Plenum, New York, 1986.
[21] G. Alberti, U. Costantino, M. Casciola, R. Vivani, Solid State Ionics 46 (1991) 61.
[22] G. Alberti, U. Costantino, J. Mol. Catal. 27 (1994) 235.
[23] S. Allulli, C. Ferragina, A. La. Ginestra, M.A. Massucci, N. Tomassini, J. Inorg. Nucl. Chem. 39 (1977) 1043.

[24] A. Hayashi, H. Nakayama, M. Tsuhako, Bull. Chem. Soc. Jpn. 75 (9) (2002) 1991.
[25] A. Boultif, D. Loueï, J. Appl. Crystallogr. 24 (1991) 987.
[26] J. Rodriguez-Carvajal, Collected Abstract of Powder Diffraction Meeting, Toulouse, France, 1990, p. 127.
[27] G.M. Sheldrick, SHELXS-86: Structure Solving Program, University of Goettingen, Germany, 1986.
[28] G.M. Sheldrick, SHELXL-93: Crystal Structure Refinement, University of Goettingen, Germany, 1993.
[29] H.M. Rietveld, Acta Crystallogr 22 (1967) 151.
[30] C.E. Bamberger, G.M. Begun, O.B. Cavin, J. Solid. State Chem. 73 (1988) 317.
[31] A. Robertson, J.G. Fletcher, J.M.S. Skakle, A.R. West, J. Solid. State Chem. 109 (1994) 53.
[32] R.D. Shannon, Acta Crystallogr. A 32 (1976) 751.
[33] S. Barth, R. Olazcuaga, P. Gravereau, G. Le Flem, P. Hagenmuller, Mater. Lett. 16 (1993) 96.
[34] R. Olazcuaga, J.M. Dance, G. Le Flem, J. Derouet, L. Beaury, P. Porcher, A. EL Bouari, A. El Jazouli, J. Solid State Chem. 143 (1999) 224.
[35] Y. Yong, P. Wenqin, Mat. Res. Bull. 25 (7) (1990) 841.
[36] S. Senbhagaraman, T.N. Guru Row, A.M. Umarji, J. Mater. Chem. 3 (1993) 309.
[37] K.C. Sobha, K.J. Rao, J. Solid State Chem. 121 (1996) 197.
[38] C. Schmutz, E. Basset, P. Barboux, J. Phys. III France 3 (1993) 757.
[39] A. El Jazouli, S. Krimi, B. Manoun, J.P. Chaminade, P. Gravereau, D. De Waal, Ann Chim. Sci. Mat. 23 (1998) 7.
[40] M.J. Bushiri, V.P. Mahadevan Pillai, R. Ratheesh, V.U. Nayar, J. Phys. Chem. Solids 60 (1999) 1983.
[41] C.E. Bamberger, G.M. Begun, J. Less-common Metals 134 (2) (1987) 201.
[42] M. Chakir, A. El Jazouli, J.P. Chaminade, F. Bouree, D. de Waal, J. Solid State Chem. 179 (1) (2006) 18.